

# Molecular Modeling of Environmentally Important Processes: Reduction Potentials

Anne Lewis and John A. Bumpus

Department of Chemistry, University of Northern Iowa, Cedar Falls, IA 50614

Donald G. Truhlar\* and Christopher J. Cramer\*\*

Department of Chemistry and Supercomputing Institute, University of Minnesota, Minneapolis, MN 55455-0431;

\*truhlar@umn.edu, \*\*cramer@pollux.chem.umn.edu

## Introduction and Pedagogical Observations

At the recent turn of the century, it was stated (1) that:

Computational Chemistry has come of age. With significant strides in computer hardware and software over the last few decades, computational chemistry has achieved full partnership with theory and experiment as a tool for understanding and predicting the behavior of a broad range of chemical, physical and biological phenomena.

There are a variety of indicators that support the above assertion and attest to the importance of this area of chemistry, not the least of which was the 1998 Nobel Prize to John Pople and Walter Kohn. Several journals are dedicated exclusively to computational chemistry and molecular modeling, and the number of articles in less specialized journals that deal with this area continues to increase. Perhaps most interesting is that more and more chemists who are not computational chemists by training or research interest have come to appreciate the use of tools provided by this discipline to help solve problems in their own areas of experimental expertise.

Clearly computational chemistry and molecular modeling have progressed to the point that undergraduate chemistry departments need to seriously consider how they will integrate this area of chemistry into an already rigorous curriculum. One way to do this would be to follow the example of the University of Nottingham in the United Kingdom, where a B.Sc. in chemistry with computational chemistry focus is now offered (2). Few undergraduate chemistry departments have the personnel or resources to make so large a commitment; however, it certainly *is* possible to develop computational laboratory exercises that can be introduced seamlessly into existing undergraduate curricula. Indeed, this *Journal* has been a leader in publishing summaries of such activities (3–11).

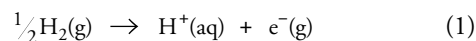
In this article, we focus on the degree to which computational quantum chemistry is finding increasing use in the modeling of environmentally important processes. This relatively new development has been spurred in part by recent advances in theoretical modeling of chemical reactions taking place in condensed phases, for example, in aqueous media (12–14). Here, we illustrate how to employ computational quantum mechanics to predict oxidation–reduction potentials for solutes in an aqueous medium (15–17).

Our focus is thus on the prediction of a *thermochemical* quantity. To that end, we will discuss in some detail (i) how to construct appropriate thermochemical cycles for the prediction of specific equilibrium constants, (ii) what physical

phenomena are represented by various legs of the thermochemical cycles, and (iii) how theoretical models may best be employed to compute accurate values for particular elementary processes. We believe that the detailed theoretical treatment will be of use to those interested in introducing such materials into appropriate undergraduate chemistry courses (e.g., physical chemistry, analytical chemistry, electrochemistry, environmental chemistry).

## Normal Hydrogen Electrode Potential

We begin with an example that relies solely on experimental data. In particular, let us consider the half-cell potential corresponding to the normal hydrogen electrode (NHE). The NHE half-reaction is defined as

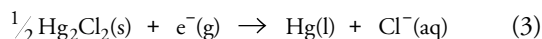


and its half-cell potential  $E^\circ$  is related to the free energy change  $\Delta G^\circ$  from left to right by the Nernst equation for the special case of all species being at their unit standard-state concentrations.

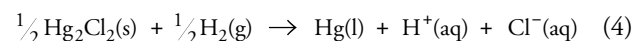
$$E^\circ = -\frac{\Delta G^\circ}{nF} \quad (2)$$

where  $n$  is the number of electrons generated in the half-reaction and  $F$  is the Faraday constant (the negative of the charge on one mole of electrons). The potential is expressed in units of volts (V; for free energies expressed in typical units,  $F$  is equal to 23.061 kcal mol<sup>-1</sup> V<sup>-1</sup> or 96.487 kJ mol<sup>-1</sup> V<sup>-1</sup>).

The free energy change for eq 1 corresponds to what is called an “absolute” potential, because it involves the generation or consumption of a free electron. Historically, absolute potentials were not readily amenable to measurement, so that electrochemical tables of redox potentials tend to list “relative” half-cell potentials. That is, a different half-cell reaction, for example,



is added to the first so that the sum of the two reactions includes no free electrons on either side. Thus, adding eqs 1 and 3, we have



The free energy change for eq 4 may be measured straightforwardly, in which case, since it is the sum of the free energy changes for eqs 1 and 3, we may employ it in the Nernst

equation to compute the potential for eq 3 *relative* to eq 1. In modern electrochemistry, the NHE is taken as zero on the relative electrochemical scale, so the entire free energy change for eq 4 is assigned as the relative potential for eq 3.

To compute the NHE *absolute* potential, we need first to give some thought to the meaning of the standard-state symbol appearing on the free energy and potential symbols in eq 2 (i.e., the superscript “o”). That superscript is meant to specify a great deal about the electrochemical system, including the phases of the chemical species (g for gas, l for pure liquid, aq for aqueous solution), their concentration in the various phases, [e.g., 1 mol per 24.5 L for gases (corresponding to 1 atm pressure for an *ideal* gas) and 1 mol per 1 L (i.e., 1 M) for aqueous solutes], the temperature (298 K), and a choice of reference zeros for atomic and molecular heats of formation.<sup>1</sup> Let us make the standard-state conventions more clear by consideration of the thermochemical cycle in Figure 1, which will prove useful for computing the absolute NHE potential.

The upper horizontal leg of the cycle in Figure 1 represents the purely gas-phase process of H–H bond rupture and subsequent hydrogen atom ionization. In order to compute the gas-phase free energy change, we must compute the free energies of all of the individual species. In this instance the 298 K heats of formation and entropies are known in every case, and they are listed in Table 1. Since H<sub>2</sub>(g) is the elemental standard state, it has a heat of formation of 0.0 kJ mol<sup>-1</sup> at all temperatures. For electrochemistry, the usual standard-state convention is to consider the free electron *also* to have a heat of formation of 0.0 kJ mol<sup>-1</sup> at all temperatures—this is called the thermal electron convention. However, another common convention exists that is known as the ion convention. In the ion convention, the electron has a heat of formation of zero only at 0 K. Since the free energy *change* of any half-reaction is a constant irrespective of standard-state convention, this implies that atomic and molecular ions must

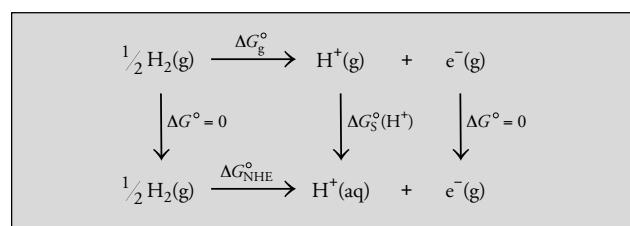


Figure 1. Thermodynamic cycle for the determination of the absolute potential of the normal hydrogen electrode.

**Table 1. Gas-Phase Thermochemical Data for Use with Equation 1, T = 298 K**

Species	$\Delta H_{f,298}^{\circ}$ / (kJ mol <sup>-1</sup> )	$S_{298}^{\circ}$ / (J mol <sup>-1</sup> K <sup>-1</sup> )	$\Delta G_{f,298}^{\circ}$ / (kJ mol <sup>-1</sup> )
H <sub>2</sub>	0.0	130.7	-39.0
H <sup>+</sup>	1536.4	109.0	1503.9
e <sup>-</sup>	0.0	20.9	-6.2

NOTE: Data are taken from the NIST Chemistry Webbook, <http://webbook.nist.gov> (accessed Jan 2004) and correspond to the thermal-electron standard state.

have 298 K heats of formation that differ under the two conventions by quantities equal to the thermal contributions to the enthalpy of one or more electrons at 298 K. An ideal gas of one mole of electrons has enthalpy  $(5/2)RT$  (see below), where  $R$  is the universal gas constant, so the difference between the two conventions is  $(5/2)qRT$ , where  $q$  is the signed charge on the ion in atomic units. Thus, tabulations of the proton heat of formation that adopt the ion convention will list 1530 kJ mol<sup>-1</sup>, while Table 1, which uses the thermal electron convention, lists 1536.4 kJ mol<sup>-1</sup>. In practice, there is no particular virtue in the choice of one standard state over another, but one must be careful to ensure use of a *consistent* convention in all related calculations.

Using the data in Table 1, we may compute 298 K free energies of formation (also listed in Table 1) as,

$$\Delta G_{f,298}^{\circ} = \Delta H_{f,298}^{\circ} - 298S_{298}^{\circ} \quad (5)$$

we can compute the free energy change as 1517.1 kJ mol<sup>-1</sup> for the gas-phase process at the top of the cycle in Figure 1. Next consider the process at the bottom of the cycle in Figure 1, which is the NHE half-reaction shown in eq 1. Since the hydrogen molecule and the free electron are defined by eq 1 to be gas phase, we need only transfer the proton from the gas phase to aqueous solution to generate the NHE half-reaction (the lower horizontal leg of the cycle in Figure 1). The free energy for such a process is called the free energy of aqueous solvation. Tissandier et al. (18) recently extrapolated gas-phase ion cluster data to arrive at a free energy of solvation for the proton of -1104.5 kJ mol<sup>-1</sup>. This value, however, derives from gas-phase measurements, so the standard-state proton concentration remains a constant during the solvation process. The thermodynamic cycle of Figure 1, however, requires the proton to go from a gas-phase concentration of 1 mol per 24.5 L to an aqueous solute concentration of 1 M. The free energy change associated with compressing an ideal gas<sup>2</sup> from 24.5 L to 1 L is  $RT\ln(24.5)$ , or 7.9 kJ mol<sup>-1</sup>. Thus, in Figure 1 the appropriate proton free energy of solvation to employ is -1096.6 kJ mol<sup>-1</sup>.

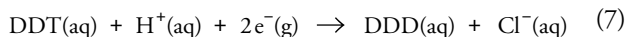
Since free energy is a state function, we may then compute the NHE free energy change from Figure 1 as the sum of the free energy changes for the bottom-to-top left vertical process (0.0 kJ mol<sup>-1</sup>, since no phase or standard-state change is involved), the left-to-right upper horizontal process (1517.1 kJ mol<sup>-1</sup>) and the top-to-bottom right vertical processes (-1096.6 and 0.0 kJ mol<sup>-1</sup>), all of which sum to 420.6 kJ mol<sup>-1</sup>. This value employed in eq 2 gives an absolute half-cell potential of -4.36 V (note that this differs from the previous standard value of -4.44 V computed by Trasatti (19) because the proton solvation free energy was less accurately known in 1986). Note that the sign of the absolute potential depends on the direction in which the reaction is written: the absolute oxidation potential of the hydrogen electrode is negative while the absolute reduction potential is positive.

## Computed Half-Cell Potentials

### Gas-Phase Calculations

In the environment, chlorinated organic compounds often undergo reductive dechlorination (17, 20, 21), a process that may render an individual environmental contaminant either more or less dangerous. Consider the case of the

pesticide DDT, which is 1,1-bis(4-chlorophenyl)-2,2,2-trichloroethane (Figure 2). For reductive dechlorination, one is potentially interested in both one-electron and two-electron processes, where the former generates a chloride ion and an organic radical, and the latter further reduces the organic radical to a carbanion that is typically protonated in water to generate a new neutral closed-shell organic molecule. That is



In this case, neither the heats of formation, nor the entropies, nor the solvation free energies of DDT, DDX, or DDD are known. However, we may employ quantum mechanics to *compute* the necessary thermochemical quantities (14, 22), and again it is helpful to proceed via a thermochemical cycle (Figures 3 and 4), since computational quantum chemistry is most powerful when applied to gas-phase processes.

To compute the enthalpy and entropy of a molecule by quantum mechanics, we must resort to a number of approximations, some of which turn out to be very mild, whereas others may sometimes introduce significant error. For simplicity, let us begin by considering an example molecule that exists as only a single conformer, for example,  $\text{H}_2$ . We may imagine building up the 298 K enthalpy of  $\text{H}_2$  in a stepwise fashion. At first glance, this endeavor may sound highly unusual, since  $\text{H}_2$  is, after all, the elemental standard state in most thermochemical conventions, and thus has an enthalpy of formation that is identically zero. Quantum mechanical (QM) computations, however, adopt a different standard state that is more convenient for the calculations; in particular, one takes bare nuclei and bare electrons, all infinitely separated and at rest, to be the relevant standard state, and this state is assigned to zero on the energy scale.

Now, from thermodynamics we have that

$$H = U + PV \quad (8)$$

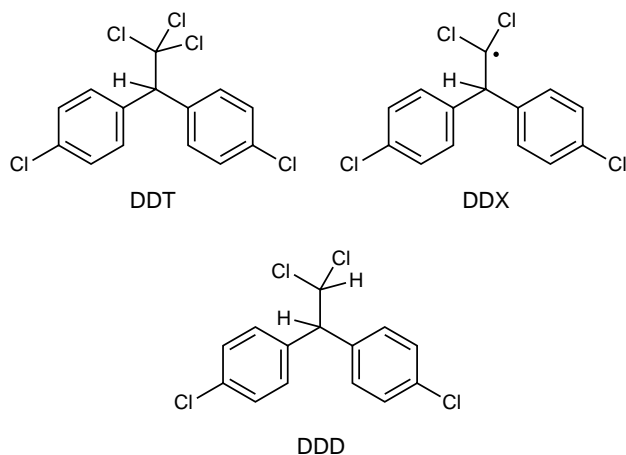


Figure 2. DDT and its one-electron (DDX) and two-electron (DDD) products.

where  $U$  is the internal energy,  $P$  is the pressure, and  $V$  is the volume. At 0 K, the internal energy of a molecule relative to the QM standard state is largely the energy associated with assembling all of the nuclei and electrons into a configuration that makes the energy as low as possible; that is, all of the electrons occupy the lowest energy orbitals that they can (generating the ground electronic state) and the nuclei adopt a geometry that minimizes the molecular energy. This “binding” energy is precisely what is computed by most modern computational chemistry programs (after optimization of the molecular geometry). It is usually called the electronic energy,  $E_{\text{elec}}$  and it includes nuclear repulsion, electron kinetic energy, electron–electron repulsion, and electron–nucleus attractions. It is typically reported in hartrees ( $E_h$ ), where 1  $E_h$  is 627.51 kcal mol<sup>-1</sup> or 2625.5 kJ mol<sup>-1</sup>. In addition, because of the Heisenberg uncertainty principle, bonds in molecules must vibrate even at 0 K, and the energy associated with bond-length, bond-angle, and torsional and out-of-plane vibrations is referred to as zero-point vibrational energy (ZPVE). That is

$$U_0 = E_{\text{elec}} + \text{ZPVE} \quad (9)$$

To compute zero-point vibrational energy, we assume that all of the vibrations in a molecule behave as quantum mechanical (QM) harmonic oscillators. In that case, ZPVE can be computed as

$$\text{ZPVE} = \sum_{m=1}^{3N-3-J} \frac{1}{2} h c \nu_m \quad (10)$$

where  $h$  is Planck’s constant,  $c$  is the speed of light, and  $\nu$  is the normal mode vibrational frequency of mode  $m$  (in wave number units) calculated by the QM harmonic oscillator approximation. The sum in eq 10 runs over all of the molecular normal modes, of which there are  $3N-3-J$  where  $N$  is the number of atoms in the molecule and  $J = 2$  for a linear molecule and  $J = 3$  for a nonlinear one (monatomic species ob-

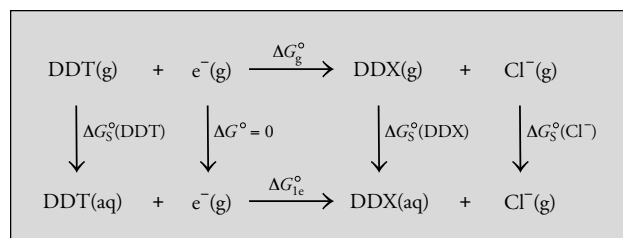


Figure 3. Thermodynamic cycle for the determination of the absolute one-electron reduction potential of DDT.

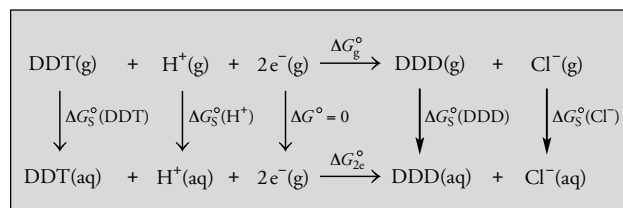


Figure 4. Thermodynamic cycle for the determination of the absolute two-electron reduction potential of DDT.

viously have no vibrations and hence no ZPVE). Efficient calculation of vibrational frequencies is possible for many different levels of QM electronic structure theory and is a standard option in modern computational chemistry packages. By employing this approach to compute ZPVE, one tacitly assumes that anharmonicity in the molecular vibrations is quantitatively unimportant, which is usually a reasonable approximation.

In the case of  $H_2$ , calculations at a fairly high level of theory (called QCISD/aug-cc-pVTZ; we will say more about levels of theory below) predict an optimized geometry having an H–H bond length of 0.743 Å, an  $E_{\text{elec}}$  of -1.17264  $E_h$ , and a vibrational frequency of 4401  $\text{cm}^{-1}$ . Thus, at this level of theory,  $U_0$  for  $H_2$  is computed from eq 9 to be -3052.4  $\text{kJ mol}^{-1}$ .

To proceed from 0 K to a nonzero temperature  $T$ , we must consider thermal contributions to  $U$ . Within the ideal gas approximation, and further assuming that we are working with molecules that do not have low-lying electronic excited states (which is the case for typical closed-shell organic molecules) and that behave as rigid rotors and have vibrations characterized as harmonic oscillators, these contributions are  $(3/2)RT$  for translation,  $(J/2)RT$  for rotation, and a vibrational contribution computed as,

$$U_{0 \rightarrow T} = R \sum_{m=1}^{3N-3-J} \frac{hc\nu_m}{k_B \left[ \exp\left(\frac{hc\nu_m}{k_B T}\right) - 1 \right]} \quad (11)$$

where  $k_B$  is Boltzmann's constant. Finally, if we assume ideal gas behavior, we may use the ideal gas law to replace  $PV$  in eq 8 with  $RT$ , so that  $H_{298}$  for  $H_2$  will be  $U_0$  plus  $(7/2)RT$  plus the contribution from vibration computed using eq 11; this sum is -3043.8  $\text{kJ mol}^{-1}$ .<sup>3</sup>

To proceed to compute the free energy  $G_{298}^\circ$ , we must compute the entropy  $S_{298}^\circ$ . The entropy has electronic, translational, rotational, and vibrational components. Under the single-electronic-state, rigid-rotator, harmonic-oscillator approximation, these may be computed in a straightforward fashion from the spin multiplicity (i.e., singlet, doublet, triplet, etc.), the molecular mass, the principal moments of inertia and rotational symmetry number, and the vibrational frequencies; relevant formulae are compiled elsewhere (14, 22, 23). Note that all of the required rotation and vibration information is available from a frequency calculation performed for the optimized geometry. Note also that the magnitude of the translational entropy depends on the specification of a standard-state concentration—most computational chemistry packages adopt the 1 mol per 24.5 L standard state. In the case of  $H_2$ , the QCISD level used thus far predicts  $S_{298}^\circ$  to be 130.3  $\text{J mol}^{-1} \text{K}^{-1}$ . Note how well this compares with the experimental value listed in Table 1—computed entropies are often quite good even from modest levels of electronic structure theory. The only important caveat is that the entropy of a QM harmonic oscillator goes to infinity as the vibrational frequency goes to zero, so molecules computed to have very low vibrational frequencies will be predicted to have entropies that may be significantly too large under the harmonic oscillator approximation. Typically such low frequency vibrations are better modeled as hindered or

free rotors, which have finite entropies, and relevant analytical formulas for such cases are available (24, 25). In addition, the popular level of molecular orbital theory known as Hartree–Fock (HF) theory tends systematically to overestimate vibrational frequencies by about 10% (14, 26). For highly accurate work, scaling factors to improve the quality of computed vibrational frequencies from a number of electronic structure levels have been determined (6, 14, 27–30).

To finish the  $H_2$  example, then, at the QCISD level we predict a  $G_{298}^\circ$ , of -3082.6  $\text{kJ mol}^{-1}$ . If we reconsider the upper leg of the thermodynamic cycle in Figure 1 using exclusively computed values, we need only compute  $G_{298}^\circ$ , for the proton and the electron to determine  $\Delta G_{298}^\circ$ , for the reaction. Since the bare proton and electron at rest have energies of zero on the QM electronic structure scale, the only contributions to their free energy are from translation<sup>4</sup> and, in the case of the electron, from doublet spin degeneracy; thus, no electronic structure calculation is involved. Using the mass of the proton and the electron and the spin degeneracy of the electron, we can compute  $G_{298}^\circ$ , values for these species of -26.2 and 0.0  $\text{kJ mol}^{-1}$ , respectively.<sup>5</sup> We thus compute  $G_{298}^\circ$  for the gas phase atomization or ionization process to be 1515.0  $\text{kJ mol}^{-1}$  [ = -26.2 + 0.0 - (1/2)(-3082.6) ], which compares quite favorably with the experimental value of 1517.1 noted above.

Let us now consider DDT and its degradation products. There is one more complicating factor now that was not an issue for  $H_2$ , namely, that these larger molecules potentially have more than one stable conformation.<sup>6</sup> For very careful work, the calculation of  $G^\circ$  for the population of conformers characterizing a molecule should be computed as,

$$G^\circ\{X\} = -RT \ln \left[ \sum_{x_i \in \{X\}} e^{-\left(\frac{G^\circ(x_i)}{RT}\right)} \right] \quad (12)$$

where  $\{X\}$  is the set of all energy-minimized molecular conformations that are characterized by unique sets of internal coordinates  $x_i$  (e.g., bond lengths, angles, and dihedrals) (31). In many cases, however, it introduces relatively little error to simply work with only the lowest-energy conformer and ignore the Boltzmann averaging implicit in eq 12.<sup>7</sup> Figure 5 illustrates the particular conformations of DDT, DDX, and DDD that were employed here.

At this point, we must decide on a level of electronic structure theory to apply to the gas-phase legs of our thermochemical cycles. As a very rough rule, the more accurate a given level of theory, the more expensive it is in terms of computational resources. Since computational resources are inevitably finite, a primary skill of the practicing computational chemist is to identify levels of theory that best balance cost and accuracy. A complete discussion being outside the scope of this article, we will indulge here in some useful generalizations. For molecules the size of DDT and its congeners, the most efficient choice for a theoretical level is density functional theory (DFT; refs 14, 32, 33), which computes molecular energetics from optimized electron densities. The key assumption is that the electronic energy is a functional of the electron density; various functionals are denoted by acronyms associated with the names of their developers, and in this article we will use a popular “hybrid” functional<sup>8</sup>

named B3LYP (34–37). The QCISD level that was used above is “quadratic configuration interaction with single and double excitations,” a more conventional approach in that it is based on electronic wave functions rather than densities.<sup>9</sup>

In addition to choosing a level of theory, one needs to specify choice of a “basis set” to carry out an electronic structure calculation. A basis set is a set of available three-dimensional functions that are used to approximate the electronic orbitals (in calculating the wave function or density) similar to the way that sine and cosine functions may be used as a basis to approximate an arbitrary one-dimensional function in Fourier analysis. Given that analogy, it should be clear that the more functions one has, that is, the bigger and more flexible the basis set, the more accurate one may expect the calculation to be. Of course, one wants to pick the functions judiciously to ensure efficiency, and an obvious choice is to use functions optimized for atoms as a basis, since we may think of a molecule as being composed of constituent atoms whose intrinsic electronic structures adjust to the molecular environment. Given such a choice, as a very rough rule one typically wants to have at a minimum two basis functions for every available valence atomic orbital<sup>10</sup> and an additional set of functions on each heavy atom having angular momentum one quantum number higher than the highest valence orbital, for example, a set of d functions on carbon.<sup>11</sup> Such a basis set is referred to as a *polarized split-valence* basis set; an example of such a basis that we will use here is one named 6-31G(d) (14, 26).<sup>12</sup>

Having explained the “level of theory” and the need for a basis set, we note that computational chemists usually just say “level” to denote a *combination* of level of theory and basis. Some molecular properties place less stringent requirements on the level than do others. Thus, for instance, reasonably good molecular geometries and vibrational frequencies (and hence thermochemical contributions) may be available from the B3LYP/6-31G(d) level, but electronic energies (i.e.,  $E_{\text{elec}}$ ) may *not* be particularly good. However, to compute an energy *without* geometry optimization is a comparatively simple task, so that often one resorts to “single-

point” calculations, where a better calculation is done for a geometry optimized at a lower level. In the case of DFT, typically one does not change the functional for the single-point calculation, but simply improves the basis set. Here, we will carry out single-point calculations at the B3LYP/6-311+G(d) level. The basis set in this case has *three* functions for each valence atomic orbital, and also adds a set of very loose valence functions (indicated by the “+” in the basis set name) that are usually very important for the computation of accurate energies for anions. The usual notation for single-point calculations of the variety described here is B3LYP/6-311+G(d)//B3LYP/6-31G(d), where the double slash separates the single-point level on the left from the geometry-optimization level on the right. Note that the level to the right of the two solids is also used to compute ZPVE and, if needed, to compute thermal contributions to the thermodynamical quantities of interest.

The choices one is forced to make in choosing a level are somewhat arbitrary. Therefore, it is usually a good first step to benchmark the theoretical choice against some known, relevant experimental quantity that may be used to judge the adequacy of the level. In the present case, we may consider first the electron affinity (EA) of the chlorine atom. Electron affinity is the difference in  $U_0^\circ$  between a neutral and its anion (recall that at 0 K the electron is defined to have  $U_0^\circ = 0$ ). The experimental EA of Cl has been measured as 348.3 kJ mol<sup>-1</sup> (39), and at the B3LYP/6-311+G(d) level it is computed to be 355.8 kJ mol<sup>-1</sup>. To additionally test the adequacy of the lower level for computing ZPVE, we may also consider the EA of the hydroxyl radical HO. In this case, the experimental EA has been measured as 167.0 kJ mol<sup>-1</sup> (39), and at the B3LYP/6-311+G(d)//B3LYP/6-31G(d) level it is computed to be 176.3 kJ mol<sup>-1</sup>. We will here consider the computed EAs to be sufficiently accurate to warrant further use of the B3LYP/6-311+G(d)//B3LYP/6-31G(d) level. Further validation of the use of DFT to compute electron affinities is available in recent articles (40–42).

The computational values necessary to compute  $\Delta G^\circ$  for the upper legs of the thermochemical cycles in Figures 3 and 4 are contained in Table 2. Using these data we compute the gas-phase one- and two-electron processes to have  $\Delta G^\circ$  values of -106.7 and -1769.4 kJ mol<sup>-1</sup>, respectively. To compute the lower legs, as in the NHE example we need to add to these values the differential solvation free energies of all aqueous products and reactants.<sup>13</sup>

### Solvation Calculations

Several models exist for the computation of free energies of solvation (14). Among the most efficient are “continuum” solvation models (43), which model the surrounding solvent as a homogeneous dielectric medium in which a reaction field is generated; the reaction field is the electric field or resulting force field that the solvent exerts on the solute after the solvent is polarized by the charge distribution of the solute. In QM calculations, the effect of this field on the electronic structure is calculated in a “self-consistent reaction-field” (SCRF) computation. Here, we employ solvation model 5.42R (44), a “generalized-Born” continuum solvation model (43), using a parameterization specific for water in conjunction with the DFT method named BPW91/6-31G(d) (45). Most continuum solvation models compute solvation free en-

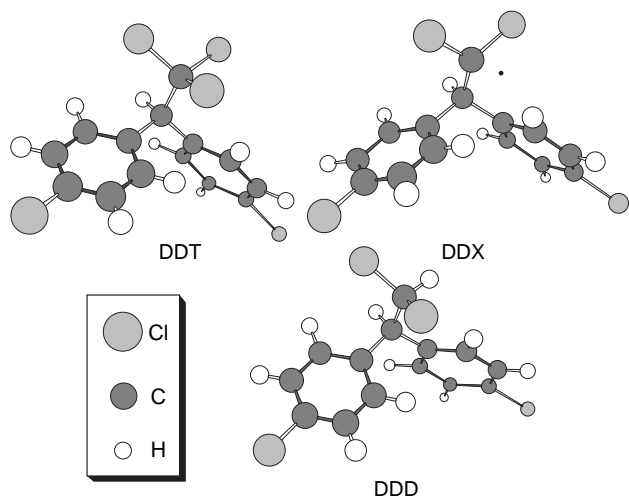


Figure 5. Optimized geometries of DDT, DDX, and DDD from which the data in Table 2 were determined.

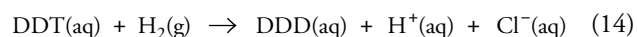
**Table 2. Computed 298 K Gas-Phase Thermochemical Data ( $E_h$ ) for Use with Equations 6 and 7**

Species	$E_{elec}$	$U_0^\circ$	$H_{298}^\circ$	$G_{298}^\circ$	$\Delta G_s^\circ$
$e^-$	0.00000	0.00000	0.00236	-0.00001	n/a
$H^+$	0.00000	0.00000	0.00236	-0.00999	-0.41766
$Cl^-$	-460.303727	-460.30373	-460.30137	-460.30231	-0.11973
DDT	-2840.13786	-2839.94728	-2839.92881	-2839.99554	-0.00195
DDX	-2379.87231	-2379.68479	-2379.66739	-2379.73386	-0.00110
DDD	-2380.53053	-2380.32966	-2380.31233	-2380.37716	-0.00275

NOTE: Gas-phase data from B3LYP/6-311+G(d)//B3LYP/6-31G(d) calculations with 1 mol per 24.5 L and ion convention standard state; solvation free energies from SM5.42R/BPW91/6-31G(d) calculations including correction to 1 M standard state.

ergies assuming the same solute concentration in the gas phase as in the condensed phase, but recall that since our gas-phase data employ a 1 atm standard state and our condensed-phase data a 1 M standard state, we must account for the free energy change associated with the increased concentration in the condensed phase ( $7.9 \text{ kJ mol}^{-1}$ ) as previously described above. The corrected SM5.42R/BPW91/6-31G(d) solvation free energies are provided in Table 2. Using these data to compute the necessary product–reactant differential solvation free energies, we determine aqueous absolute half-cell free energy changes of  $-418.8$  and  $-989.2 \text{ kJ mol}^{-1}$ , respectively.

As noted above, experiment typically measures not the absolute cell potential, but rather the relative cell potential. That is, eqs 6 and 7 are added to eq 1 taken once and twice, respectively, to create the complete electrochemical cells



and the  $\Delta G^\circ$  values for eqs 13 and 14 are used in the Nernst equation to compute the reduction potentials for eqs 6 and 7 relative to the NHE. By construction,  $\Delta G^\circ$  for eqs 13 and 14 comes simply from summing the computed absolute half-cell free energy changes listed above with  $420.6 \text{ kJ mol}^{-1}$  and  $841.1 \text{ kJ mol}^{-1}$ , respectively, these being the experimentally known one- and two-electron free energy changes for the NHE. The relevant values are then  $1.8$  and  $-148.1 \text{ kJ mol}^{-1}$  for  $\Delta G^\circ$  for eqs 13 and 14, respectively.

However, prior to using these free energies in the Nernst equation, one last standard-state issue must be addressed. Recall that we are working with a 1 M standard state for aqueous solutes. Experimentally, however, aqueous reductive dechlorinations are by convention (46) buffered to pH 7 (i.e., a proton concentration of  $10^{-7} \text{ M}$ ) and the  $Cl^-$  concentration is held at  $10^{-3} \text{ M}$ . In order to convert from one standard-state convention to another, we may use

$$\Delta G^{\circ'} = \Delta G^\circ + RT \ln \left( \frac{Q^{\circ'}}{Q^\circ} \right) \quad (15)$$

where  $Q$  is the reaction quotient (i.e., the ratio of concentrations that appear in the equilibrium constant) evaluated with all species at their standard-state concentrations and expressed so that the argument of the logarithm is dimensionless. If

we take superscript “o'” as the pH 7 and  $10^{-3} \text{ M}$   $Cl^-$  convention and superscript “o” as the all aqueous concentrations at 1 M convention, this leads, for eq 6, to

$$\Delta G^{\circ'} = \Delta G^\circ + RT \ln \frac{\left[ \frac{(1 \text{ M DDX})(10^{-3} \text{ M Cl}^-)}{(1 \text{ M DDT})} \right]}{\left[ \frac{(1 \text{ M DDX})(1 \text{ M Cl}^-)}{(1 \text{ M DDT})} \right]} \quad (16)$$

from which one can quickly see that a correction factor of  $RT \ln(10^{-3})$  or  $-17.1 \text{ kJ mol}^{-1}$  must be applied to the original free energy ( $^\circ$ ) to convert to the alternate standard state ( $^{\circ'}$ ). Examination of eq 7 makes it clear that a correction of  $22.8 \text{ kJ mol}^{-1}$  should be applied to that case. This leads to final  $\Delta G^{\circ'}$  values of  $-15.4$  and  $-125.3 \text{ kJ mol}^{-1}$  for eqs 13 and 14, respectively.

### Putting It All Together

The values computed above from summing the top and side legs of the relevant thermodynamic cycles, when used in eq 2, yield relative reduction potentials for eqs 6 and 7 of  $0.16$  and  $0.65 \text{ V}$ , respectively.

### Concluding Remarks

Although this paper is written from the pedagogical standpoint of illustrating the steps involved in computing a reduction potential, we now stop to ask how accurate these example reduction potentials are likely to be. An interesting comparison may be made to the analogous one- and two-electron reductive dechlorinations that convert hexachloroethane (HCA) to pentachloroethane (i.e., the identical process to that for DDT, but the diarylmethine group is replaced with trichloromethyl). In that case, experimental one- and two-electron reduction potentials have been measured to be  $0.11$  and  $0.67 \text{ V}$  (46), and a DFT method very similar to that employed here predicts values of  $0.44$  and  $0.69 \text{ V}$  (17). From this comparison and related experience (17), we infer that (i) the DFT method is more likely to be robust for the two-electron process than for the one-electron process, with the latter potentially being predicted to be too positive by about  $0.3 \text{ V}$ , and (ii) the reductive dechlorination of DDT proceeds with very similar energetics to the analogous process for HCA, that is, trichloromethyl and bis(4-chlorophenyl)methyl mani-

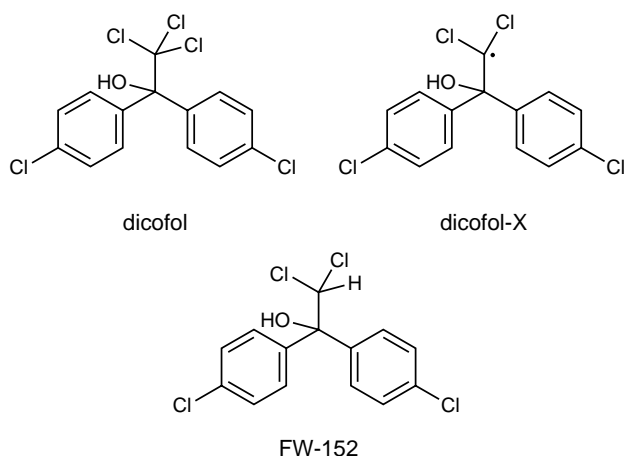


Figure 6. Dicofol and its one-electron (dicofol-X) and two-electron (FW-152) products.

fest similar substituent effects on an adjacent trichloromethyl group undergoing reductive dechlorination.

It is important to emphasize that what we are calculating here are well defined thermodynamic quantities that correspond to reversible processes under nearly equilibrium conditions. In actual practice one may encounter overpotentials and other nonthermodynamic complications associated with irreversible processes like reductive dechlorination, and one must always be careful to ascertain the extent to which experimentally measured quantities differ from calculated reversible values. As final food for chemical thought, we consider the reductive dechlorination of dicofol to FW-152 (Figure 6). This process is nearly identical to the reductive dechlorination of DDT, except that the hydrogen atom on the doubly benzylic position has been replaced with an hydroxyl group. Using the additional data in Table 3, the reader may wish to verify that, in the conventional reductive-dechlorination standard state ( $^{\circ}$ ), the reduction potentials for the one- and two-electron processes are 0.15 and 0.72 V, respectively, relative to the NHE. Thus, replacing hydrogen by an electron-withdrawing hydroxyl group is predicted to render the two-electron reduction process more favorable by 0.07 V but to have little effect on the one-electron process.

In closing, we note that thermodynamic cycles analogous to those used here are also often used in the *ab initio* computation of acidity constants (i.e.,  $pK_a$ 's) (3, 43, 47). Prediction of aqueous acidity constants can also be important in modeling environmentally relevant chemical phenomena.

## Software and Computational Details

All calculations reported in this work were carried out with the Gaussian 98 suite of electronic structure programs (48) augmented by the solvation package MN-GSM (49). While MN-GSM is not yet publicly distributed, its functionality is available in the HONDOPLUS (50, 51) and GAMESSPLUS (52) program packages (53). In this article, the single-point DFT calculations on the largest molecules with the largest basis sets took roughly 20 hours of CPU time on a modern workstation processor. Similar to slightly longer quantities of time were required for geometry optimizations of the various large molecules using smaller basis sets. All of the calculations related to DDT and its degradation products were completed over the course of approximately eight weeks by an undergraduate chemistry student initially having no familiarity with computational chemistry.

## Acknowledgments

AL and JAB received support from the National Science Foundation under Grant No. NSF/CHE-0137438 (REU Site Award). We thank Bethany Kormos for technical assistance in carrying out some of the calculations.

## Notes

1. The standard-state symbol may or may not imply that the thermodynamic quantities refer to hypothetical ideal gases and hypothetical ideal solutions. Here, we will not explicitly discuss nonideality.
2. This is actually a special case of the more general procedure required to convert between standard states that is discussed in more detail in the context of eq 15.
3. Note that an ideal gas of 1 mol of electrons has enthalpic contributions only from translation and the  $PV$  term:  $(5/2)RT$ .
4. As monatomic species they neither rotate nor vibrate.
5. The value of 0.0 for the electron with this choice of temperature and standard state results simply from accidental cancellation of the different terms.
6. Stable conformation in the sense of there being a local minimum in the molecular potential energy surface.
7. Inspection of eq 12 should make clear that if a single isomer is substantially lower in free energy than all of the others, then at reasonable temperatures the population free energy is indeed essentially equal to that conformer's free energy—thus it is always worth some effort to do the best job possible of determining the lowest-energy conformer, the *global minimum*.
8. The functional is referred to as hybrid because it includes some character from HF theory (14, 26) in addition to DFT.

Table 3. Computed 298 K Gas-Phase Thermochemical Data ( $E_h$ ) for Reductive Dechlorination of Dicofol

Species	$E_{\text{elec}}$	$U_0^{\circ}$	$H_{298}^{\circ}$	$G_{298}^{\circ}$	$\Delta G_s^{\circ}$
Dicofol	-2915.36820	-2915.17403	-2915.15454	-2915.22261	-0.00557
Dicofol-X	-2455.10482	-2454.91303	-2454.89569	-2454.95996	-0.00523
FW-152	-2455.76435	-2455.55962	-2455.54132	-2455.60728	-0.00822

NOTE: Gas-phase data from B3LYP/6-311+G(d)//B3LYP/6-31G(d) calculations with 1 mol per 24.5 L and ion convention standard state; solvation free energies from SM5.42R/BPW91/6-31G(d) calculations including correction to 1 M standard state.

9. QCISD is a key component in the Gaussian-2 work (38) that contributed to J. A. Pople's Nobel prize.

10. A single basis function is usually sufficient for core orbitals.

11. Remember that these are *functions not orbitals*, so it should not be misconstrued that the use of such functions somehow implies carbon d orbitals are "occupied" in the electronic configuration.

12. The basis 6-31G(d) is also called 6-31G\* in older literature.

13. An alternative way to carry out the calculations would have been to use energies of formation, enthalpies of formation, and free energies of formation. This would involve introducing the elements in their standard states, but since all such data must ultimately cancel in a balanced chemical reaction that would simply have complicated the calculations. The route taken here is preferred when dealing with data from QM electronic-structure calculations.

## Literature Cited

- Truhlar, D. G.; McKoy, V. *Comput. Sci. Eng.* **2000**, *26*, 19–21.
- University of Nottingham, School of Chemistry, Prospective Undergraduate Student. <http://www.nottingham.ac.uk/chemistry/undergraduate/prospective/compchem.html> (accessed Jan 2004).
- Pietro, W. J. *J. Chem. Educ.* **1994**, *71*, 416–420.
- Pfennig, B. W.; Frock, R. L. *J. Chem. Educ.* **1999**, *76*, 1018–1022.
- Gasyňa, Z. L.; Rice, S. A. *J. Chem. Educ.* **1999**, *76*, 1023–1029.
- McClain, B. L.; Clark, S. M.; Gabriel, R. L.; Ben-Amotz, D. *J. Chem. Educ.* **2000**, *77*, 654–660.
- Graham, K. J.; Skoglund, K.; Schaller, C. P.; Muldoon, W. P.; Klassen, J. B. *J. Chem. Educ.* **2000**, *77*, 396–397.
- Lipkowitz, K. B.; Robertson, D. *J. Chem. Educ.* **2000**, *77*, 206–209.
- Whisnant, D. M.; Howe, J. J.; Lever, L. S. *J. Chem. Educ.* **2000**, *77*, 199–201.
- Cook, A. G.; Kreeger, P. K. *J. Chem. Educ.* **2000**, *77*, 90–92.
- Cramer, C. J.; Kormos, B. L.; Winget, P.; Audette, V. M.; Beebe, J. M.; Brauer, C. S.; Burdick, W. R.; Cochran, E. W.; Eklov, B. L.; Giese, T. J.; Jun, Y.; Kesavan, L. S. D.; Kinsinger, C. R.; Minyaev, M. E.; Rajamani, R.; Salsbury, J. S.; Stubbs, J. M.; Surek, J. T.; Thompson, J. D.; Voelz, V. A.; Wick, C. D.; Zhang, L. *J. Chem. Educ.* **2001**, *78*, 1202–1205.
- Structure and Reactivity in Aqueous Solution*; Cramer, C. J., Truhlar, D. G., Eds.; ACS Symposium Series; Vol. 568; American Chemical Society: Washington DC, 1994.
- Quantitative Treatments of Solute/Solvent Interactions*; Politzer, P., Murray, J. S., Eds.; Elsevier: Amsterdam, 1998.
- Cramer, C. J. *Essentials of Computational Chemistry: Theories and Models*; Wiley: Chichester, United Kingdom, 2002.
- Reynolds, C. A. *Int. J. Quantum Chem.* **1995**, *56*, 677–687.
- Winget, P.; Weber, E. J.; Cramer, C. J.; Truhlar, D. G. *Phys. Chem. Chem. Phys.* **2000**, *2*, 1231–1239.
- Patterson, E. V.; Cramer, C. J.; Truhlar, D. G. *J. Am. Chem. Soc.* **2001**, *123*, 2025–2031.
- Tissandier, M. D.; Cowen, K. A.; Feng, W. Y.; Gundlach, E.; Cohen, M. H.; Earhart, A. D.; Coe, J. V.; Tuttle, T. R. *J. Phys. Chem. A* **1998**, *102*, 7787–7794.
- Trasatti, S. *Pure Appl. Chem.* **1986**, *58*, 955–966.
- Vogel, T. M.; Criddle, C. S.; McCarty, P. L. *Environ. Sci. Technol.* **1987**, *21*, 722–736.
- Schwarzenbach, R. P.; Angst, W.; Holliger, C.; Hug, S. J.; Klausen, J. *Chimia* **1997**, *51*, 908–914.
- Computational Thermochemistry: Prediction and Estimation of Molecular Thermodynamics*; Irikura, K., Frurip, D. J., Eds.; ACS Symposium Series; Vol. 677; American Chemical Society: Washington, DC, 1998.
- Fay, J. A. *Molecular Thermodynamics*; Addison-Wesley: Reading, MA, 1965.
- Pitzer, K. S.; Gwinn, W. D. *J. Chem. Phys.* **1942**, *10*, 428–440.
- Truhlar, D. G. *J. Comp. Chem.* **1991**, *12*, 266–270.
- Hehre, W. J.; Radom, L.; Schleyer, P. v. R.; Pople, J. A. *Ab Initio Molecular Orbital Theory*; Wiley: New York, 1986.
- Pople, J. A.; Scott, A. P.; Wong, M. W.; Radom, L. *Israel J. Chem.* **1993**, *33*, 345–350.
- Scott, A. P.; Radom, L. *J. Phys. Chem.* **1996**, *100*, 16502–16513.
- Wong, M. W. *Chem. Phys. Lett.* **1996**, *256*, 391–399.
- Lynch, B. J.; Truhlar, D. G. *J. Phys. Chem. A* **2001**, *105*, 2936–2945.
- Ben-Naim, A. *Statistical Thermodynamics for Chemists and Biochemists*; Plenum: New York, 1992; p 421–430.
- Kohn, W.; Becke, A. D.; Parr, R. G. *J. Phys. Chem.* **1996**, *100*, 12974–12980.
- Koch, W.; Holthausen, M. C. *A Chemist's Guide to Density Functional Theory*; Wiley-VCH: Weinheim, Germany, 2000.
- Becke, A. D. *Phys. Rev. A* **1988**, *38*, 3098–3100.
- Lee, C.; Yang, W.; Parr, R. G. *Phys. Rev. B* **1988**, *37*, 785–789.
- Becke, A. D. *J. Chem. Phys.* **1993**, *98*, 5648–5652.
- Stephens, P. J.; Devlin, F. J.; Chabalowski, C. F.; Frisch, M. J. *J. Phys. Chem.* **1994**, *98*, 11623–11627.
- Curtiss, L. A.; Raghavachari, K.; Trucks, G. W.; Pople, J. A. *J. Chem. Phys.* **1991**, *94*, 7221–7230.
- Trainham, R.; Fletcher, G. D.; Larson, D. J. *J. Phys. B* **1987**, *20*, L777–784.
- Rienstra-Kiracofe, J. C.; Tschumper, G. S.; Schaefer, H. F., III; Nandi, S.; Ellison, G. B. *Chem. Rev.* **2002**, *102*, 231–282.
- Bauschlicher, C. W.; Gutsev, G. L. *Theor. Chem. Acc.* **2002**, *108*, 27–30.
- Jensen, F. *J. Chem. Phys.* **2002**, *117*, 9234.
- Cramer, C. J.; Truhlar, D. G. *Chem. Rev.* **1999**, *99*, 2161–2200.
- Hawkins, G. D.; Cramer, C. J.; Truhlar, D. G. *J. Phys. Chem. B* **1998**, *102*, 3257–3271.
- Zhu, T.; Li, J.; Hawkins, G. D.; Cramer, C. J.; Truhlar, D. G. *J. Chem. Phys.* **1998**, *109*, 9117–9133.
- Totten, L. A.; Roberts, A. L. *Crit. Rev. Environ. Sci. Technol.* **2001**, *31*, 175–221.
- Liptak, M. D.; Shields, G. C. *Int. J. Quantum Chem.* **2001**, *85*, 727–741.
- Frisch, M. J.; Trucks, G. W.; Schlegel, H. B.; Scuseria, G. E.; Robb, M. A.; Cheeseman, J. R.; Zakrzewski, V. G.; Montgomery, J. A.; Stratmann, R. E.; Burant, J. C.; Dapprich, S.; Millam, J. M.; Daniels, A. D.; Kudin, K. N.; Strain, M. C.; Farkas, O.; Tomasi, J.; Barone, V.; Cossi, M.; Cammi, R.; Mennucci, B.; Pomelli, C.; Adamo, C.; Clifford, S.; Ochterski, J.; Petersson, G. A.; Ayala, P. Y.; Cui, Q.; Morokuma, K.; Salvador, P.; Dannenberg, J. J.; Malick, D. K.; Rabuck, A. D.; Raghavachari, K.; Foresman, J. B.; Cioslowski, J.; Ortiz, J. V.; Baboul, A. G.; Stefanov, B. B.; Liu, G.; Liashenko, A.; Piskorz, P.; Komaromi, I.; Gomperts, R.; Martin, R. L.; Fox, D. J.; Keith, T.; Al-Laham, M. A.; Peng, C. Y.; Nanayakkara, A.; Challacombe, M.; Gill, P. M. W.; Johnson, B.; Chen, W.;



- Wong, M. W.; Andres, J. L.; Gonzalez, C.; Head-Gordon, M.; Replogle, E. S.; Pople, J. A. *Gaussian 98 Revision A.10*; Gaussian, Inc.: Pittsburgh, PA, 2001.
49. Xidos, J. D.; Li, J.; Thompson, J. D.; Hawkins, G. D.; Winget, P. D.; Zhu, T.; Rinaldi, D.; Liotard, D. A.; Cramer, C. J.; Truhlar, D. G.; Frisch, M. J. *MN-GSM*, version 2.2; University of Minnesota: Minneapolis, MN, 2002.
50. Nakamura, H.; Xidos, J. D.; Thompson, J. D.; Li, J.; Hawkins, G. D.; Zhu, T.; Lynch, B. J.; Volobuev, Y.; Rinaldi, D.; Liotard, D. A.; Cramer, C. J.; Truhlar, D. G. *HONDOPLUS*, version 4.4; University of Minnesota: Minneapolis, MN, 2003; based on *HONDO*, version 99.6.
51. Dupuis, M.; Marquez, A.; Davidson, E. R. *HONDO 99.6*; 1999; based on *HONDO 95.3*; Dupuis, M.; Marquez, A.; Davidson, E. R. Quantum Chemistry Program Exchange QCPE; Indiana University, Bloomington, IN 47405.
52. Pu, J.; Thompson, J. D.; Xidos, J. D.; Li, J.; Zhu, T.; Hawkins, G. D.; Chuang, Y.-Y.; Fast, P. L.; Liotard, D. A.; Rinaldi, D.; Cramer, C. J.; Truhlar, D. G. *GAMESSPLUS*, version 4.1; University of Minnesota: Minneapolis, MN, 2004.
53. *HONDOPLUS* and *GAMESSPLUS* software program packages are freely distributed. Details are available at the University of Minnesota Solvation Models and Software Home Page. <http://comp.chem.umn.edu/solvation> (accessed Jan 2004).

## Corrections

**J. Chem. Educ.** 2004, **81**, 596–603

On page 597 of the article “Molecular Modeling of Environmentally Important Processes: Reduction Potentials” (1), we incorrectly stated that the free energy of solvation of the proton,  $-1104.5$  kJ/mol, reported by Tissandier et al. (2) in 1998, corresponds to the same concentration in the gas phase and in liquid solution. Actually, their reported result corresponds to the standard state of 1 atm in the gas phase and 1 M in solution. Therefore it is not appropriate to make any correction to their measured value, as was done in our article to arrive at a 1 atm to 1 M transfer free energy of  $-1096.6$  kJ/mol. Note that this implies that the absolute potential of the standard hydrogen electrode is 4.28 V, not 4.36 V. In addition, there is an error in the 298 K free energy of the chloride anion in Table 2 on p 601; the correct value is  $-460.31875 E_{\text{h}}$  (3).

**Literature Cited**

1. Lewis, A.; Bumpus, J. A.; Truhlar, D. G.; Cramer, C. J. *J. Chem. Educ.* **2004**, *81*, 596–603.
2. Tissandier, M. D.; Cowen, K. A.; Fendg, W. Y.; Gundlach, E.; Cohen, M. H.; Earhart, A. D.; Coe, J. V.; Tuttle, T. R. *J. Phys. Chem. A* **1998**, *102*, 7787–7794.
3. Cramer, C. J.; Truhlar, D. G. In *Trends and Perspectives in Modern Computational Science*, Lecture Series on Computer and Computational Sciences, Vol. 6. Maroulis, G.; Simos, T. E., Eds.; Brill Academic: Amsterdam, 2006; pp 112–140.

**Anne Lewis and John A. Bumpus**

Department of Chemistry  
University of Northern Iowa  
Cedar Falls, IA 50614

**Donald G. Truhlar and Christopher J. Cramer**

Department of Chemistry and Supercomputing Institute  
University of Minnesota  
Minneapolis, MN 55455-0431